1887 Microsc. Microanal. 21 (Suppl 3), 2015
doi:10.1017/S1431927615010211 Paper No. 0942 

# Prospects for Detecting Single Vacancies by Quantitative Scanning Transmission Electron Microscopy

Jie Feng[1], Alexander V. Kvit[2], Andrew B. Yankovich[1,2], Chenyu Zhang[1,2], Dane Morgan[1,2], Paul M. Voyles[1,2]

[1.] Materials Science Program, University of Wisconsin-Madison, Madison, WI, 53706, USA
[2.] Department of Materials Science and Engineering, University of Wisconsin-Madison, Madison, WI, 53706, USA

Transmission electron microscopy (TEM) and scanning TEM (STEM) have made significant advances in direct imaging of point defects, including substitutional impurities, interstitial impurities, and self-interstitials. However, imaging defects that decrease, rather than increase local intensity, such as vacancies, remains a significant challenge. Here we show in simulations that recent advances in highly quantitative, picometer-precision STEM imaging [1] may make it possible to detect single cation vacancies in a complex oxide both through the reduction of the column intensity and the small shifts in the neighboring atomic column positions.

We use frozen phonon simulations to explore if vacancies in $LaMnO_3$ perovskites can be imaged in the STEM [2]. At least 128 phonon configurations are required to ensure sub-picometer special precision and lower than 1% intensity fluctuations in simulations of 20 nm thick [100] $LaMnO_3$. Simulation parameters were set based on a probe-corrected FEI Titan STEM at 200 kV. The probe convergence semi-angle was 24.5 mrad and the detector inner angles were 84.4 mrad and 8.48 mrad for high-angle annular dark-field (HAADF) STEM and annular bright field (ABF) STEM, respectively.

Figure 1(a) shows the 3D structure of $LaMnO_3$ (*Pnma* space group) and the 2D projection along [100]. There are two symmetry distinct near-neighbor La column separations along the *x* direction and one along the *y* direction. Figure 1(c) shows the vacancy visibility, defined as the percent reduction in intensity of vacancy-containing column with respect to a perfect column, which is 3% ~ 9% for a single La vacancy in a 10 nm thick sample and 1% ~ 6% visibility in a 15 nm thick sample. Figure 1(d) and (e) show that all three inter-column separations are measurably changed by a single La vacancy in both HAADF image and ABF image, and that all separation changes depend on the vacancy depth. The depth dependence may make it possible to not only detect a single La vacancy, but also accurately localize its depth. A similar analysis predicts a 1% ~ 3% reduced intensity and pm-scale contraction/expansion caused by a single Mn vacancy under the same conditions. The depth dependencies of vacancy introduced visibility and column displacements are likely caused by electron channeling effects [3]. The predicted changes are within the detection limitations of HAADF STEM imaging in experiment, which can now achieve sub-picometer precision and 1% intensity sensitivity by non-rigid registration and averaging of an image series [1]. Overall, these results predict that single cation vacancy imaging is possible in $LaMnO_3$.

Experiments, performed on [100] $LaMnO_3$ film grown on $DyScO_3$ substrate, have identified candidate La vacancies in STEM images, as shown in Figure 2. Detailed comparison of experiment and simulations may in the future enable full, 3D reconstruction of the defect structure in $LaMnO_3$.

References:

[1] A. B. Yankovich, et al., Nat. Commun. **5** (2014), p. 4155.
[2] E.J. Kirkland in "Advanced Computing in Electron Microscopy", 1st Edition, Springer, 1998.
[3] P. M. Voyles, et al., Ultramicroscopy. **96** (2003), p. 251.
[4] This work was supported by the US Department of Energy, Basic Energy Sciences, Grant DE-FG02-08ER46547.

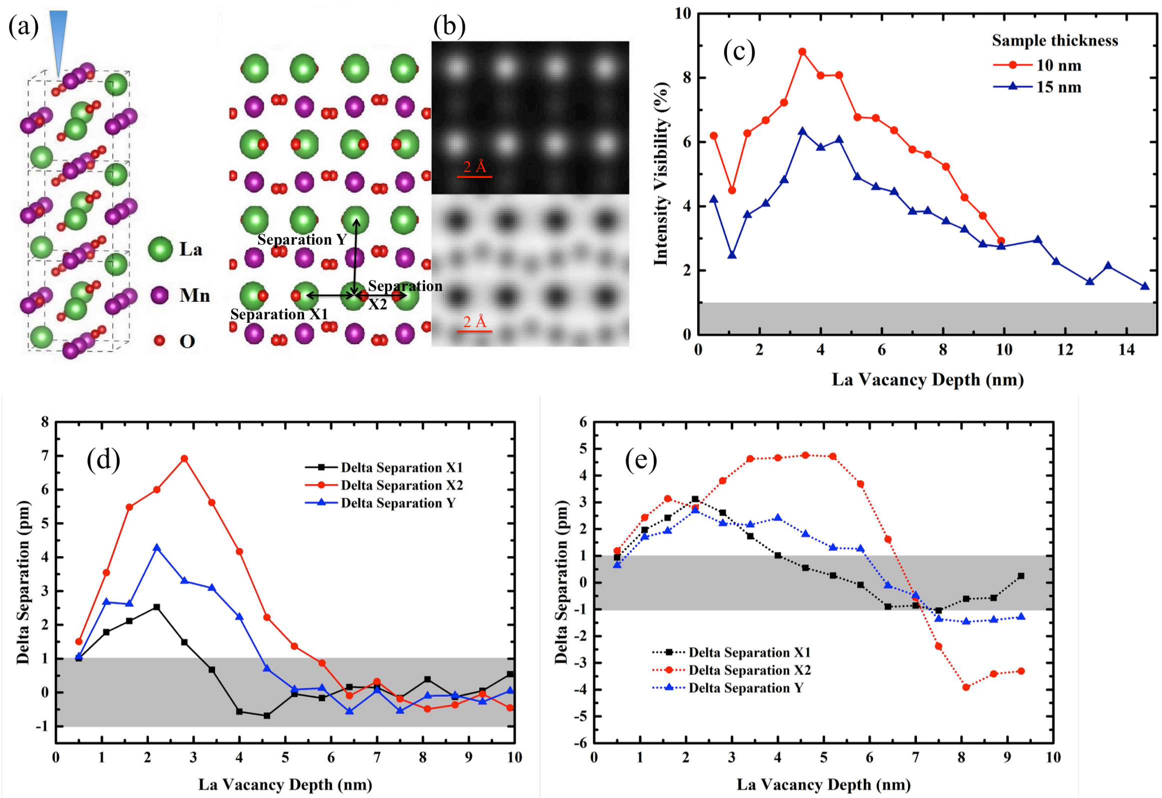


**Figure 1.** Simulations for $LaMnO_3$ [100]: (a) unit cell in perspective (left) and 2D projection (right). (b) Simulated HAADF (top) and ABF (bottom) images. (c) Intensity visibility for $V_{La}$ as a function of vacancy depth for two STEM sample thicknesses. (d) Atomic column displacements in a 10 nm thick sample from HAADF images. (e) Atomic column displacements in a 10 nm thick sample from ABF images. Data inside shaded regions are not detectable. Separations are defined in (a).

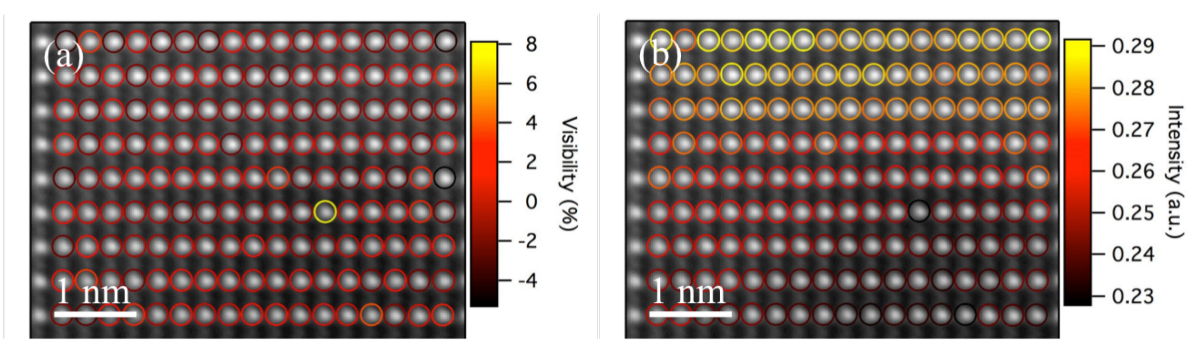


**Figure 2.** Experimental HAADF images of [100] $LaMnO_3$: (a) visibility map and (b) intensity map. The column marked in the red box is likely to contain a single La vacancy.